On-Filter Integration of Soot Oxidation and Selective Catalytic Reduction of NOx with NH3 by Selective Two Component Catalysts

On-filter integration of soot oxidation and selective catalytic reduction of NO_x with NH_3 by selective two component catalysts

Authors:

Ferenc Martinovic, Tahrizi Andana, Fabio Alessandro Deorsola*, Samir Bensaid, Raffaele Pirone

Politecnico di Torino, Department of Science Applied and Technology, Corso Duca degli Abruzzi 24, 10129 – Torino, Italy.

Corresponding Author:

* Fabio Alessandro Deorsola

Department of Applied Science and Technology, Politecnico di Torino, Corso Duca degli Abruzzi 24, 10129 Torino, Italy.

Tel.: +39 011 0904662; fax: +39 011 0904699; E-mail address: fabio.deorsola@polito.it

Acknowledgements

This work was funded through a SINCHEM Grant. SINCHEM is a Joint Doctorate programme selected under the Erasmus Mundus Action 1 Programme (FPA 2013-0037).

Abstract

A group of catalysts were developed with the purpose of enhancing the soot oxidation in the SCR-on filter (SCRoF) system, without negatively effecting the NO_x conversion associated to NH_3 oxidation. The impregnation with alkali metal of a series of supports, characterized by a lack of strong superficial acid sites, improved soot oxidation simultaneously preventing ammonia adsorption, thus its catalytic oxidation. Strong synergy was observed between a ZrO_2-CeO_2 support and potassium, decreasing the T_{50} of the soot conversion of 170 °C in loose contact. This catalyst was added to a Fe-ZSM5 SCR catalyst without negative effect for the SCR activity. The complex interaction between the potassium-based soot oxidation catalyst and SCR one was investigated. The soot-soot oxidation catalyst-SCR catalyst contact mode was found to be a key factor and the increased contact of the soot-soot oxidation catalyst is preferable. Such dual component catalyst system was demonstrated to be promising for simultaneous removal of NO_x and soot on a single filter.

Keywords: SCR on filter; soot oxidation; SCR; Fe-ZSM5

1. Introduction

Diesel engines have higher net efficiency than gasoline ones, for which their use is widespread in long haul transport, heavy work machines and passenger vehicles. The emission of NO_x and soot however remains problematic and, with more stringent regulation, the aftertreatment devices become more complex and expensive. Soot abatement remains especially challenging since oxidation with oxygen starts only at temperatures above 500 °C [1–4]. Typical exhaust temperatures, however, are in the range of 200-400 °C, and exceeding 500 °C only under maximum load or artificial conditions like active regeneration by fuel injection [1–4]. The soot oxidation temperature can be reduced by the use of the soot oxidation catalysts or through the NO_x present in the exhaust gas, NO_2 being a much stronger oxidant for soot than O_2 [1,5,6]. In the latter case, catalytic systems usually involve an active component (in most applications Pt) for NO to NO_2 oxidation, in the so called continuously

regenerating trap (CRT) [1], which is practically effective only if both NO_x levels and exhaust temperatures are within appropriate ranges, as happens for heavy duty diesel engines. However, in passenger vehicles, NO_2 is present in concentrations which are insufficient to induce appreciable soot oxidation by passive regeneration [1,4]. For this reason, active regeneration is the preferred mechanism to restore the functionality of the Diesel Particulate Filter (DPF) after reaching its limit of soot loading, which is determined by pressured drop constraints as well as the need to avoid the risk for an excessive temperature rise inside the filter [4,7,8]. It is preferable to reduce the active regeneration temperature on the DPF to avoid filter damage as well as additional high fuel consumption. For this, the filter is usually coated with a catalyst, that is capable of catalyzing soot oxidation relying mainly on oxygen. These catalysts are necessarily stable and usually based on doped cerium oxides, perovskites, Ag or alkali salt [9–12].

To achieve the latest Euro 6 regulations a section for NO_x reduction in the aftertreatment system has to be included. There are generally 2 main types of NO_x reduction systems:

1. NO_x reduction by NH_3 from decomposition of urea solution. The catalysts are mainly based on Fe or Cu zeolites or titania-supported vanadia [13,14], according to the preferred temperature ranges of application.

2. Lean NO_x Trap (LNT) catalysts which operate in alternating rich-lean regimes for NO_x capture and reduction [14].

Between these two systems, the urea-based system is preferred in some applications for the real driving emission treatment as it presents higher conversion, wider operational temperature window, considerably better stability and much lower fuel penalty (0.5% vs 2%) [14,15].

The typical aftertreatment system consists of several bricks, as well as a dedicated urea solution reservoir, with different functionalities and their integration in vehicles is highly complex and limited by space requirements (especially in light duty diesel, LDD). One way to reduce the size of the aftertreatment is to integrate diesel particulate filter and urea-mediated Selective Catalytic Reduction (SCR) of NO_x into the same device, named Selective Catalytic Reduction on Filter (SCRoF)

[4,5,8,16,17]. With this, the complexity and size are reduced and, due to close coupling, higher temperatures can be achieved enabling more efficient operation. For the SCRoF, a monolith is used with channels plugged on alternating ends, thus forcing the exhaust gas through the monolith wall, with the SCR catalyst which is located inside the filter pores. Soot is filtered and retained inside and on the wall, most of it (>80%) present on the top as soot cake. The current state-of-the-art of the SCR catalyst in the commercial SCRoF system is Cu-zeolite, more specifically Cu-chabazite, deposited inside the pores of SCRoF by BASF [4]. Cu-chabazite offers high SCR activity and hydrothermal stability however it lacks any soot oxidation capability [7,8,16,18–20]. For SCRoF, it has been shown that soot oxidation and regeneration is inhibited by the much faster SCR reaction which quickly consumes the NO_2 leaving none for soot oxidation. This leads to much faster pore clogging with soot and higher backpressure [7,8,16,18–20]. This can be presented as competing reactions R1-R3:

Fast SCR reaction: $2NH_3 + NO + NO_2 \rightarrow 2N_2 + 3H_2O$ R1

Soot oxidation by NO_2: $C + NO_2 + O_2 \rightarrow CO + NO$ R2

$2C + O_2 + 2NO_2 \rightarrow CO_2 + 2NO$ R3

Rappe [8] showed that on SCRoF the soot conversion profile was shifted upwards 70 °C in the presence of the SCR reaction compared to the case without SCR, under the same conditions. As a solution, non-uniform SCR catalyst distribution in the monolith was suggested, with the SCR catalyst concentrated in the downstream portion and a NO_2/NO_x ratio higher than 0.5. Watling, Marchitti and Kolstakis [5,7,18] also showed for SCRoF that under 450 °C the soot oxidation and filter regeneration was significantly inhibited due to NO_2 consumption and only above 450 °C the oxidation by O_2 was prevalent. It was further suggested that concentrating the catalyst in the downstream portion of the filter improved the soot oxidation activity due to smaller NO_x conversion at the inlet. As will be shown later, the NO to NO_2 oxidation and soot oxidation by NO_2 reactions cannot be used on SCRoF since the NO_2 is consumed quickly by the SCR reaction [8]. SCRoF is usually regenerated by raising the temperature above 600 °C by injecting hydrocarbons. This is undesirable since excess fuel is

consumed and elevated temperatures can irreversibly damage the filter or accelerate the ageing of the SCR catalyst [4,8].

To introduce soot oxidation function on SCRoF, and to reduce the regeneration temperature and time, a novel dual layer reactor configuration is proposed here for the first time, a so-called second generation SCR-on-filter or "SCR^2F". Dual layer monoliths have been used in diesel aftertreatment monoliths such as LNT+SCR combination [14], for widening operational window by the combination of Fe and Cu zeolite [13] and for stabilizing SCRoF with silica [21]. In the proposed SCR^2F dual layer configuration, a soot oxidation catalyst layer is situated on the top of the filter on the inlet side, in contact with the soot cake. The SCR catalyst is deposited inside the monolith like in conventional SCRoF system. Such dual layer configuration could perform both the NO_x reduction and achieve significant reduction of the soot regeneration temperature, thus reducing the associated fuel penalty, as well as mitigate the conditions that might lead to catalyst and filter damage during active regeneration.

Since the ammonia passes through the top layer first, any ammonia oxidation would be detrimental for the SCR reaction. The challenge was to find a catalyst that is highly active for soot oxidation in loose contact, however completely inactive for ammonia oxidation. It has been found that catalysts with alkali carbonates impregnated on supports with neutral or basic surface (e.g. MgO, sodalite, MgAlO, CeO_2, ZrO_2, etc.) are suitable for such purpose. In this paper, the interaction between a suitable catalyst with high soot oxidation activity and a conventional SCR catalyst (Fe-ZSM5) are also explored in a laboratory setup.

2. Experimental

2.1. Catalysts' preparation

For the soot oxidation catalyst, CeO_2-ZrO_2 (labelled CZ) with Zr:Ce atomic ratio 9:1 (Alfa-Aesar, product number 39216) was impregnated with 20 wt.% K_2CO_3 by wet impregnation: CZ was placed

in a 0.03 M aqueous solution of K_2CO_3 and stirred for 24 h and then water was evaporated at 80 °C. The obtained 20 wt.% K_2CO_3/CeO_2-ZrO_2 (KCZ) had K:Zr:Ce bulk atomic ratio 3:9:1 determined by EDS, or 8 wt.% K. CZ was chosen as the support, as after screening of several different types of potential supports (MgO, MgAlO, nepheline, CeO_2-CuO) the CZ had the best performance for soot oxidation and low ammonia oxidation. The powder was dried overnight at 100 °C and calcined at 800 °C for 5 h with a heating rate of 10 °C/min.

To demonstrate the effect of excessive NH_3 oxidation on the SCR reaction in the SCR and soot oxidation coupled reaction CZ was impregnated with 10 %wt $AgNO_3$ (Ag/CZ). Ag/CZ was chosen because of soot oxidation characteristics comparable to KCZ (see Table 1 and [12,22,23]). Other catalysts were also prepared by using different supports synthetized with different methods (MgAlO, MgO, nepheline, CeO_2-CuO) wet impregnated with 20 wt.% K_2CO_3 by employing the same procedure described previously for the KCZ catalyst. These supports were chosen after literature review and screening of several potential catalysts. The preparation of these materials are given in the supplementary material and in references [24–27].

To achieve stable performance and high NO_x conversion in a wide temperature range and because of its widespread industrial use, for the SCR reaction Fe-ZSM5 was prepared by ion exchange. First NH_4-ZSM5 (Alfa Aesar, SiO_2: Al_2O_3 = 23) was calcined at 500 °C for 3 h to transform it into H-ZSM5. H-ZSM5 was placed in a 50 mM aqueous solution of $Fe(NO_3)_3$, stirred at 50 °C for 24 hours. The slurry was then washed and dried overnight at 100 °C and calcined at 700 °C for 6 h with a heating rate of 10 °C/min. Final Fe content in the Fe-ZSM5 was determined by EDS and ICP to be 0.5 wt.%.

The soot used in the reactivity tests was a commercial Printex U carbon black from Degussa, commonly used as model soot in the scientific literature. The soot had an average particle size 25 nm (supplier specification), specific surface area 88 m^2/g and cumulative pore volume 0.31 mL/g obtained from BET measurement.

2.2. Catalyst characterization

XRD was conducted for phase verification with X'Pert Philips PW3040 diffractometer equipped with Pixel detector using a Cu Kα radiation. The diffractograms were obtained in the 2θ range 20-80° with 0.013° step size.

H_2 TPR was conducted on TRPDO-1100 equipment (Thermo Scientific) with 5% H_2 in Ar as reaction gas. Before the test, the samples were pretreated in N_2 at 550 °C and cooled to room temperature. After that, reduction was performed with 5 °C/min ramp until 850 °C. Soot TPR was performed in the reactor setup (see below) by mixing the catalyst and the soot and ball milled for 15 minutes to achieve tight contact. The temperature was increased with 5 °C/min rate in N_2 gas without oxygen.

Specific surface area was determined on Tristar II 3020 instrument (Micrometrics) by N_2 physisorption of the catalyst pretreated at 200 °C for 2 hours. The reported values (S_{BET}) were calculated according to the BET method.

Morphology and elemental composition were determined by field emission scanning electron microscopy (FESEM) using Zeiss MERLIN Gemini II equipped with EDS at 3 keV accelerating voltage and different magnifications.

NO_x temperature programmed desorption-oxidation (TPDO) was performed in the reactor (see below) on the KCZ sample to determine the NO_x adsorption capacity and reactivity. The catalyst was fully saturated with 250 ppm NO, 250 ppm NO_2, 4% O_2 in N_2 at 200 °C and desorbed with a heating rate of 5 °C/min in 4% O_2 in N_2 atmosphere with w/f 0.027 g_{cat}·s/mL. To determine the soot-NO_x-O_2 reactivity and interaction, the desorption-reaction was done in the presence and absence of soot.

NH_3 TPD was performed in the reactor (see below) by saturating the catalyst with 500 ppm NH_3 in N_2 at 100 °C and desorbed in N_2 with a 5 °C/min temperature ramp with w/f 0.027 g_{cat}·s/mL.

2.3. Catalytic tests

Catalytic tests were conducted in a 10 mm i.d. quartz tube reactor typically with 270 mg of powdered (<100 μm fraction) and/or pelletized (<300 μm fraction) catalyst placed on a porous sintered glass membrane inside the tube. The quartz reactor containing the catalyst bed was placed inside a PID-

controlled vertical oven. A thermocouple was vertically put on the top of the catalytic bed in order to track and measure the reaction temperature. In all tests, a temperature ramp of 2 °C/min was used, starting after the outlet composition stabilized at initial temperature of 200 °C (waiting time c.a. 15 minutes). Such slow ramp ensured that the NO_x and NH_3 composition was similar as in isothermal test in the observed range.

A 4-way valve was placed upstream the reactor allowing it to bypass and enabling the analysis of both inlet and outlet gas mixture through a single device. The NO, NO_2, N_2O, NH_3, CO and CO_2 species were continuously analyzed with UV (Limas 11, ABB) and NDIR (Uras 14, ABB) analyzers. The volumetric flowrate was 600 mL/min in all cases which is typically equivalent to 80 000 h^{-1} GHSV or *w/f* of 0.027 g·s/mL.

Depending on the test, different gas mixture combinations were used. In soot oxidation tests with oxygen, 270 mg of catalyst and 30 mg of soot were mixed gently with spatula to obtain loose contact and oxidized in a 4% O_2 in N_2 gas flow. Soot oxidation in the presence of NO_x was also performed, in which case 250 ppm NO and 250 ppm NO_2 was also added to the oxidizing gas. In some cases, the KCZ was saturated with NO_x (labeled KCZ-sat) at 200 °C before the reaction to reproduce steady state conditions and avoid interference between NO_x adsorption and soot reactivity.

To demonstrate the catalytic effect of KCZ on the soot-NO_x-O_2 reaction, comparative soot oxidation tests were conducted on Fe-ZSM5 and KCZ-sat in a gas mixture containing 500 ppm NO_x with initial ratio NO_2/NO_x=0.5. The non-catalytic test was performed by mixing SiC with soot under the same conditions. The SCR reaction over Fe-ZSM5 was conducted by feeding 4% O_2, 250 ppm NO, 250 ppm NO_2, 500 ppm NH_3 in N_2 over 270 mg of catalyst with and without 30 mg of soot.

The SCR conversion was calculated according to the following formula:

$$X_{NOx} = \frac{[NO_x]_{in} - [NO_x]_{out}}{[NO_x]_{in}}$$

while for the N_2 selectivity the following one was employed:

$$S_{N_2} = 1 - \frac{2[N_2O]_{out}}{[NO_x]_{in} - [NO_x]_{out} + [NH_3]_{in} - [NH_3]_{out}}$$

The temperatures when 10% 50%, 90% of soot was converted and the CO_x concentration achieved maximum conversion (T_{10}, T_{50}, T_{90}, T_{max}) were used for comparison of different catalysts and configurations and reference to non-catalytic tests. T_{10} and T_{90} are especially useful for the comparison of the onset of the soot oxidation and to evaluate the temperature at which the soot is fully oxidized. The turnover frequency of the soot oxidation was calculated according to the formula for the specific soot oxidation rate proposed in [28,29]. It was evaluated at 400 °C and expressed as normalized soot oxidation rate with the units $mg_{oxidized\ soot} \cdot s^{-1} \times g_{initial\ soot} \cdot g^{-2}_{catalyst}$. The soot oxidation reproducibility can be low in loose contact as uncertainty is involved with the mixing mode. Soot oxidation was repeated in triplets over several catalysts and the maximum change in T_{max} observed was always within ± 5 °C.

The integrated soot oxidation and NO_x SCR reactions were performed by employing 270 mg of KCZ, 270 mg of Fe-ZSM5 and 30 mg of soot with different contact and granulation modes. The flowrate of the gaseous reaction mixture was 600 mL/min and consisted of 250 ppm NO, 250 ppm NO_2, 500 ppm NH_3 and 4% O_2 in N_2.

The relative positioning of the soot oxidation and SCR catalyst was evaluated by dimensional analysis to compare the catalyst positioning in the laboratory reactor with the real-life monolith and experiments were conducted to demonstrate the importance of the contact mode and occlusion between the soot oxidation and SCR catalyst and soot. Two cases were compared in the dimensional analysis:

1. Physical mixture where the SCR and soot oxidation catalyst powders were physically mixed.
2. Dual-bed configuration with soot catalyst on top and separated with glass wool from the SCR catalyst on the bottom.

To compare the diffusive and convective fluxes, the Peclet number was evaluated. The assumptions and equations used are given in the supplementary material. At 300°C the estimated Pe number was 0.35 in the monolith, meaning that the diffusional fluxes are the main transport form of the reactant species. For the dual bed reactor configuration, with the catalyst separated in layers, the estimated Pe

number 28.32 which means that the SCR reactions in the bottom layer had no effect on the soot oxidation in the upper layer and the soot oxidation reactions were not influenced by diffusion and the SCR reaction. This drastic difference is because the wall flow velocity in the monolith is almost 7 times lower than the flow velocity in the tubular reactor [8,16]. The Pe number for the physical mixture of the two catalyst in the reactor was 0.95, slightly higher than in the monolith, but the characteristic lengths (~100 μm) and the transport mode was still in the diffusional regime and approximated the monolith quite well (see e.g. [16,18]). The lower distance between the particles in the physical mixture compared to the distance between the dual bed configuration (100 μm compared to 3 mm) enabled the diffusional operating regime in the reactor and approximated the monolithic configuration closely.

Different configurations were tested to demonstrate the influence of different contact modes, the importance of the soot catalyst-soot contact, the impact of the SCR catalyst acting as a barrier as well as the influence of diffusion and NO_x adsorption (also shown schematically on Figure 1). To do this, different granulations of the used catalysts were implemented, the "powdered" catalysts refer to finely crushed catalyst, which was easily sieved through the 100 μm sieve, while the "pelletized" fraction refer to the fraction between 300-500 μm :

1. 270 mg of pelletized KCZ mixed in loose contact with 30 mg of soot and with powdered 270 mg Fe-ZSM5 also in loose contact.
2. 270 mg of powdered KCZ and 30 mg of soot in loose contact, mixed with pelletized 270 mg of the SCR catalyst in loose contact
3. To determine the worst-case scenario for the SCR reaction, powdered 270 mg of KCZ-Sat was mixed with 30 mg of soot in loose contact and with powdered 270 mg of the SCR catalyst.
4. 270 mg of KCZ and 270 mg of Fe-ZSM5 catalyst pelletized together in tight contact and mixed with 30 mg of soot in loose contact.

5. In the dual bed reactor system, the 270 mg of Fe-ZSM5 was placed on the bottom and sealed with glass wool. In the upper layer 270 mg of KCZ-sat was mixed in loose contact with 30 mg of soot.
6. To demonstrate the negative effect of ammonia oxidation, powdered 270 mg of Ag/CZ was used as soot oxidation catalyst mixed with 30 mg of soot and 270 mg of Fe-ZSM5.

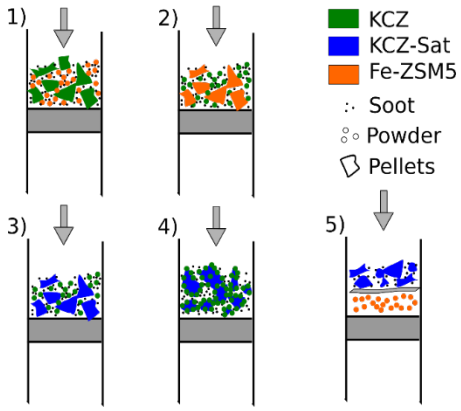

Figure 1. Schematics of different reactor configurations used for the physical mixture experiments.

While there is a lot of research reports and patents concerning the use of K in aftertreatment devices (LNT, DPNR, CRT) [9,30,31], the main issue that have prevented their wide-spread use is the low stability. To check the stability of the KCZ catalyst, the following tests were conducted:

1. Low temperature stability: repeated tests of soot combustion with O_2 were performed with the same catalyst. During each test, the temperature was allowed to reach 650°C regardless if the soot was burned completely.
2. High temperature stability in wet atmosphere: the KCZ catalyst was hydrothermally treated at 700°C for 7 h in 4 % O_2 and 5 % H_2O in N_2. This accelerated ageing is equivalent to c.a. 30 000 km of normal operation [31].

3. Results and discussion:

3.1. Characterization results

The diffractograms of the CZ and KCZ catalysts, reported in Figure S1, are practically equal suggesting that the no phase transformation occurred. The potassium carbonate phase was not detected as it was uniformly distributed on the CZ support surface and likely because of the overlapping of the main diffraction peaks of the K_2CO_3 with CZ [32]. Indeed, for potassium insertion to occur in the zirconia lattice prolonged calcination at temperatures above 900 °C is required [33]. Characteristic peaks revealed the tetragonal structure of Ce-stabilized ZrO_2 ($Zr_{0.88}Ce_{0.12}O_2$-t) as the dominant phase with smaller amount of monoclinic phase zirconia (ZrO_2-m). The average crystallite size, calculated according to the Scherrer equation, was 22.5 nm.

The FE-SEM images, shown in Figure S2, reveal uniform coating of CZ with the K_2CO_3 on the KCZ sample. After impregnation, the particle size slightly increased and the edges of the CZ became rounder as they were covered with potassium (see Figure S2A and S2B). After hydrothermal ageing, aggregates of recrystallized potassium salts were found in several spots, indicating that the hydrothermally aged catalyst had lower potassium dispersion (Figure S2C). These crystals were likely formed by the excess potassium that is not adhering strongly to the support surface.

The BET surface area and microporosity for both the CZ and KCZ samples were low, 8.51 m^2/g and 9.42 m^2/g respectively. The addition of potassium did not change significantly the surface area.

The ammonia TPD profile, reported in Figure 2A, indicates the presence of small amount of acid sites on the CZ support. However, after adding potassium on the CZ support, all the acid sites disappeared and there was no NH_3 adsorption/desorption on the sample. From this, we can infer that the acid sites (both Lewis and Bronsted) are poisoned and/or blocked by the potassium that prevents any ammonia reactivity [35]. In contrast, by adding Ag on CZ, the number of acid sites increased. In fact, a pronounced peak can be observed in the low temperature region, while the NH_3 signal quickly decreases, most likely because the adsorbed ammonia was oxidized by the Ag.

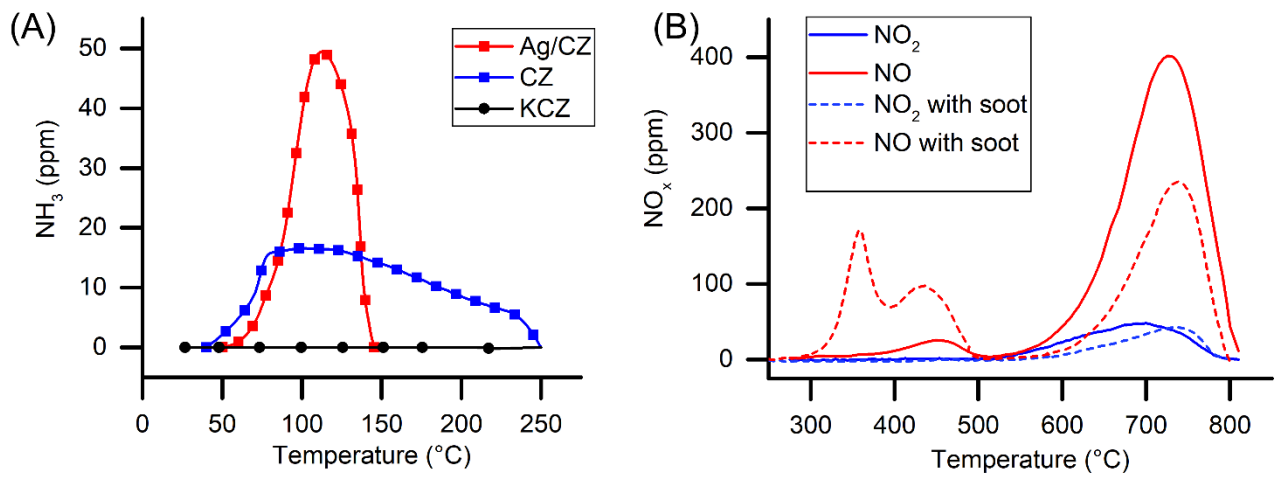

Figure 2. (A) NH_3 TPD of CZ, KCZ and Ag/CZ samples; (B) NO_x TPDO of the KCZ sample in absence (full lines) and presence (dashed lines) of soot.

In Figure 2B the NO_x TPDO of the KCZ catalyst is shown. During saturation, both NO and NO_2 were adsorbed on the sample with simultaneous evolution of CO_2, suggesting that the following reaction occurred:

$K_2CO_3 + 2\ NO_2 \rightarrow 2\ KNO_3 + CO_2$ R4

$KNO_3 \rightarrow KNO_2 + 1/2O_2$ R5

$2\ KNO_2 \rightarrow K_2O + 2NO + 1/2O_2$ R6

$2K_2NO_3 + C \rightarrow 2K_2O + CO_2 + 2NO$ R7

During NO_x TPDO, 2 peaks were identified on the KCZ-sat samples: a small peak at 450 °C of the chemisorbed nitrites, and another at 740 °C of the reactively adsorbed nitrite and nitrated potassium salts (Figure 2B) [35,36]. Complete decomposition occurred slightly above 800 °C (R6). During adsorption most of the adsorbed species on the catalyst were NO_2, forming nitrates (R4) and the adsorption of NO was minimal. While most of the adsorbed species were NO_2, NO was the main component observed during desorption. This was likely because of the nitrate decomposition into nitrite above 500 °C according to R5 [37]. When soot was added to the saturated KCZ in loose contact, the NO_x adsorption and desorption dynamics during the TPDO changed significantly, and NO_x was released at significantly lower temperatures. Additional peak was observed at much lower

temperature (at 360 °C), simultaneously accompanied with significantly higher soot combustion rates (see Figure 2B). This indicates that the NO_2 adsorbed on K has higher reactivity with soot and KCZ catalyzes not only the oxidation of soot with O_2 but also the soot-NO_2-O_2 reaction (see Figure 4 for corresponding the soot oxidation). Similar phenomena were investigated in more detail on Pt-K/Al_2O_3 [35–39], however in our case higher desorption temperature and no platinum group metal was used. The total amount of NO_x adsorbed-desorbed on the catalyst was 1.24 mmol NO_x/g_{cat} in both cases, meaning about 65% of K was present in the nitrate/nitrite form. The rest of the K is possibly in the form -O-K on the surface or covered and inaccessible for NO_x adsorption [32].

In Figure 3 the soot-TPR and H_2-TPR are shown. CZ in tight contact with soot showed small ability to generate reactive oxidizing species during soot-TPR, i.e. the oxygen mobility was low. K_2CO_3 alone, however, could oxidize higher amount of soot. The mechanism for this, suggested in [27], is:

$$C + K_2CO_3 \rightarrow CO_2 + K_2O \qquad R8$$

In [27] it was also investigated in detail the reason why K_2CO_3 impregnated on ZrO_2 and CeO_2 could oxidize higher amount of soot. The support, coupled with potassium (K^+) with high electron positivity, could destabilize the oxygen on the surface in the form of O-K bonds [35–37]. This increased the surface oxygen mobility of the support and facilitated oxygen spillover to activate the soot oxidation.

Furthermore, the activity for the Boudouard reaction or incomplete soot oxidation (R9) on potassium-containing samples was increased at temperatures above 600°C as high CO production was observed.

$$C + CO_2 \rightarrow 2CO \qquad R9$$

The enhanced reducibility of the support by potassium was further confirmed by H_2-TPR. The H_2 reduction of CZ had a single peak at 610 °C, which corresponds to the reduction of the CeO_2 to Ce_2O_3 in the sample. According to the stoichiometric calculations, the total amount of H_2 uptake (465 μmol/g) on CZ corresponded to the Ce^{4+} to Ce^{3+} reduction. While K_2CO_3 by itself was not reducible by H_2, the KCZ sample had higher H_2 uptake (761 μmol/g), nearly double the amount of the CZ sample. It is hypothesized that the addition of K enhanced the reducibility of ZrO_2, which is not

reducible by itself [38]. Visually the same color change was observed, the fresh KCZ was transformed from pale yellow to dark brown after H_2-TPR.

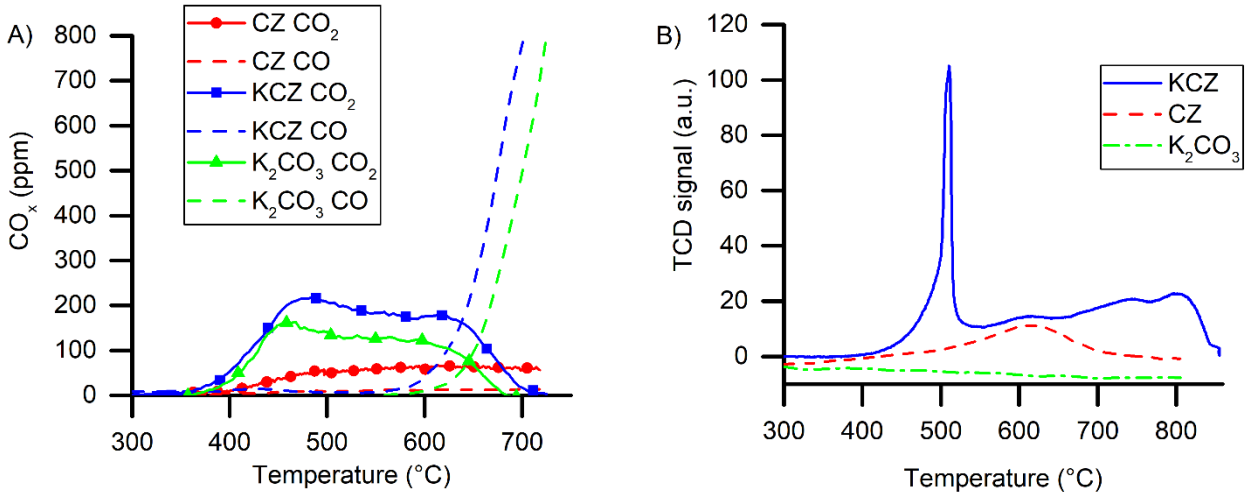

Figure 3. Soot (A) and H_2 (B) TPR of K_2CO_3, CZ and KCZ samples.

3.2. Catalytic activity of the soot oxidation catalyst

In Figure 4 and Table 1 the effect of different supports impregnated with K_2CO_3 on the oxidation of soot is compared. The CZ support demonstrated superior performance with respect to the other supports and it was chosen for further testing. Supports with redox capability (e.g. CeO_2-CuO, CeO_2-ZrO_2) had some synergistic effect with potassium, while neutral supports (e.g. MgO, MgAlO) always had worse performance than pure K_2CO_3 (see Table 1). As illustrated in Figure S3, the optimal loading was found to be 20 wt.% K_2CO_3 on CZ, while above this loading the conversion decreased. The optimal K loading amount found matches closely the reported values in literature as optimal [10,22,24,25,39,40]. As can be seen from Table 1 and Figure 4, the CZ support alone had no effect on soot oxidation in loose contact and it was practically the same as the blank test with SiC. The K_2CO_3 powder had lower soot oxidation activity than KCZ, suggesting strong interaction and synergy between the CZ support and potassium. In fact, the KCZ catalyst in loose contact had much better soot oxidation activity than the CZ support in tight contact with soot (Figure 4), i.e. the improvement of the soot oxidation activity cannot be attributed simply to enhanced contact.

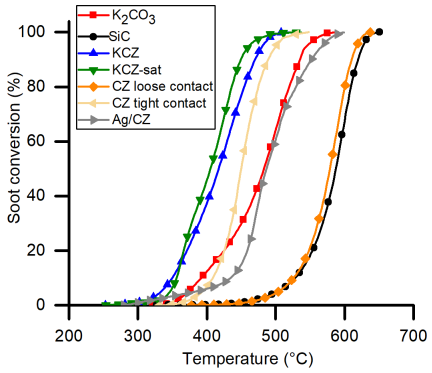

Figure 4. Soot TPO activity comparison of potassium carbonate, CZ support, KCZ and KCZ-Sat on soot oxidation. Reaction conditions: *w/f* 0.027 g_{cat}·s/mL, 4% O_2 in N_2, 9:1 catalyst:soot mass ratio, loose contact, 2 °C/min heating ramp.

Table 1. Soot oxidation characteristics of the screened catalyst active for soot oxidation with O_2. Reaction conditions same as in Fig.4.

Catalyst	T_{10} [°C]	T_{50} [°C]	T_{max} [°C]	T_{90} [°C]	CO_2 selectivity[a] [%]	Specific soot oxidation rate[c]
SiC	528	587	594	620	51	0
CZ loose contact	526	579	586	610	63	0
CZ tight contact	408	450	443	489	91	1.25
K_2CO_3	391	483	497	536	88	1.13
KCZ-Sat	355	405	425	448	95	2.83
KCZ-Sat[b]	354	391	356	433	95	3.2
10% K_2CO_3/CZ	407	470	472	526	92	1.53
20% K_2CO_3/CZ (KCZ)	348	417	429	470	93	2.91
30% K_2CO_3/CZ	412	475	478	534	93	1.99
40% K_2CO_3/CZ	418	488	498	540	91	0.71
20% K_2CO_3/MgAlO	473	524	526	570	92	0.14
20% K_2CO_3/MgO	471	537	544	571	78	0.12
20%K_2CO_3/Nepheline	475	536	544	569	79	0.17
20% K_2CO_3/CeO_2-CuO	430	448	494	540	98	0.40
Ag/CZ	434	485	469	552	99	0.28

[a]CO_2 selectivity at T_{max}, selectivity changes little (±2%) during the reaction.
[b]In this case the reaction gas also contained 250 ppm NO and 250 ppm NO_2.
[c]The specific soot oxidation rate was calculated at 400 °C and expressed as [$mg_{oxidized\ soot} \cdot s^{-1} \times g_{initial\ soot} \cdot g^{-2}_{catalyst}$]

KCZ-Sat had higher activity than KCZ, however this was due to the effect of NO_x present on the catalyst. The KCZ catalyzes the reaction between the adsorbed NO_x and soot since the presence of soot improved the release of NO_x on KCZ-Sat (see Figure 2B), which is accompanied by high soot oxidation rates (Figure 4). The mechanism of the soot oxidation over cerium and doped cerium oxides was investigate extensively in literature by different methods. It is generally accepted that the oxidation of the soot and NO is initiated with the activation and adsorption of gas phase oxygen on the surface, which is subsequently transferred to the reacting species [11,28,29,41]. The promoting effect of potassium on this catalytic cycle is still disputed, however the evidence points for the electron transfer mechanism (e.g. [9,25,27]), proved by UPS and FTIR. Potassium, due to its high electron positivity, enhances the electron transfer between the support surface and the molecule receiving it. In the case of potassium doping it is still disputed if oxygen receives the electron forming reactive gaseous oxidative radicals (e.g. CO_3^{2-}, O_2^{2-}) or it is directly transferred to soot [9, 22, 25-27, 35]. To demonstrate the catalytic effect of KCZ on the soot-NO_x-O_2 reaction, comparative soot oxidation tests were conducted on Fe-ZSM5 and KCZ-sat in a gas mixture containing 500 ppm NO_x with initial ratio of NO_2/NO_x 0.5. The difference in the NO_2/NO_x ratio on Fe-ZSM5 and KCZ indicates the rate and efficiency of NO_2 utilization for soot oxidation. This is illustrated in Figure S4, where the NO_2/NO_x ratio during the soot oxidation with NO_x is much lower in the presence of KCZ than on Fe-ZSM5. Fe-ZSM5 has no catalytic effect for soot oxidation with NO_2 (see e.g. [18] and Figure S5) meaning that the NO_2 is reacting with the soot from the gas phase and the NO_2/NO_x ratio during the soot oxidation remains always higher than 0.25. NO_2 however, becomes more reactive with soot in presence of KCZ and during the reaction almost all the NO_2 is effectively utilized for soot oxidation. With potassium the NO_2 is adsorbed and activated becoming more reactive with soot. This was also confirmed with the NO_x TPDO in the presence of soot, as illustrated in Figure 2B.

For the application of the dual layer, it is necessary that the soot oxidation catalyst is not oxidative towards ammonia and allows the SCR reaction to proceed. Over the KCZ and over catalysts described in Table 1, neither ammonia adsorption nor oxidation in O_2 and $O_2 + NO_x$ atmosphere was observed.

The NH_3 oxidation started at temperatures higher than 500 °C and it was practically the same as the non-catalytic oxidation (Figure S5). This was achieved by tailoring the catalyst surface properties as the potassium poisoned the acid sites on the catalyst and prevented ammonia adsorption and activation thereby reaction (see Figures S2 and S5 and [34]). In contrast, the CZ support and the Ag/CZ catalyst had high ammonia conversion and NO production.

3.3. Catalytic activity of SCR catalyst

For the SCR catalyst the Fe-ZSM5 catalyst was chosen because of high NO_x conversion in wide operational temperature range, as it has been investigated in detail in the scientific literature and because of its widespread commercial use [13,42–44]. Cu zeolite was not used as at higher temperatures the NO_x conversion decreased and ammonia oxidation was more pronounced [8,13,17,18,44]. As illustrated in Figure 5A, Fe-ZSM5 had no catalytic effect on the soot oxidation in oxygen and was the same as the non-catalytic oxidation. In the presence of NO_x, the soot oxidation by the gas phase NO_2 started already at low temperatures (T_{10} = 384 °C) however the soot oxidation rate was rather slow due to limited NO_x availability. However, using the same reaction conditions and in the presence of NH_3, the oxidizing effect of NO_2 was lost due to much faster NO_2 consumption by the fast SCR and the soot conversion showed the same profile as the soot oxidation in only O_2. This finding is important, since it indicates that soot oxidation mediated by NO_2 cannot be applied on SCRoF and for the SCR^2F configuration, as NO_x is consumed in the SCR reaction and not available for soot oxidation.

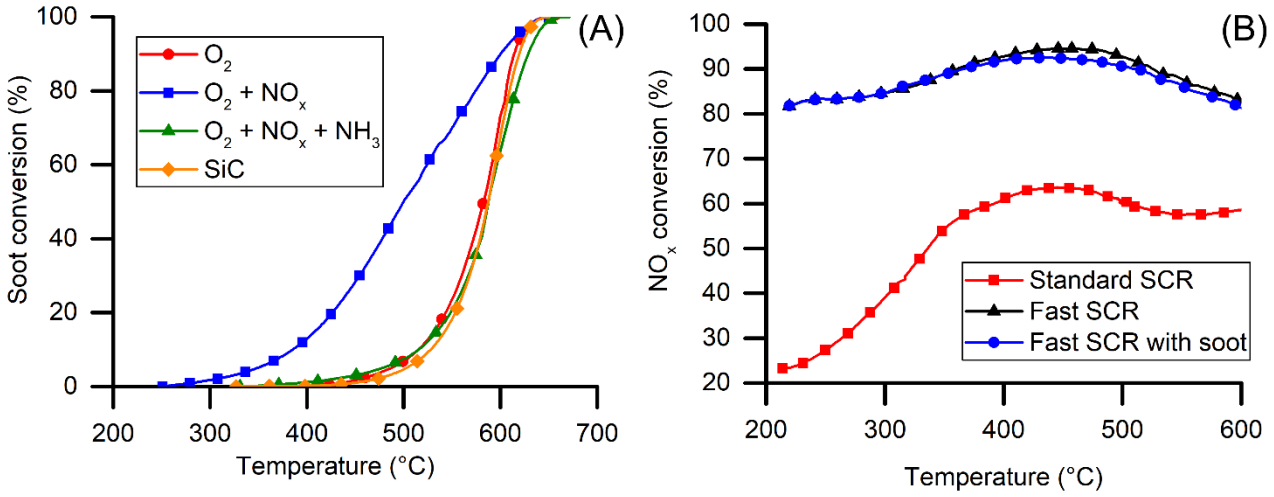

Figure 5. (A) Soot TPO on Fe-ZSM catalyst with different gas composition. Reaction conditions: *w/f* 0.027 g_{cat}·s/mL, 4% O_2 in N_2, 9: 1 catalyst: soot mass ratio, loose contact, 2 °C/min heating ramp. When indicated, 250 ppm NO, 250 ppm NO_2 and 500 ppm NH_3 was also added; (B) SCR activity of Fe-ZSM5. Reaction conditions: *w/f* 0.027 g_{cat}·s/mL, 500 ppm NO_x (NO_2/NO_x = 0 for standard SCR and 0.5 for fast SCR), 500 ppm NH_3, 4% O_2 in N_2, 9:1 Fe-ZSM5:soot mass ratio, loose contact, 2 °C/min heating ramp.

Table 2. Soot oxidation on Fe-ZSM5 in different gas compositions. Reaction conditions same as in Figure S5.

Gas composition	T_{10} [°C]	T_{50} [°C]	T_{max} [°C]	T_{90} [°C]	CO_2 selectivity[a] [%]
O_2	515	583	594	613	52
O_2+NO+NO_2	384	500	516	600	72
O_2+NO+NO_2+NH_3	517	584	605	629	48
SiC	528	587	594	620	51

[a]CO_2 selectivity at T_{max}

Fe-ZSM5 had very good fast-SCR performance in the observed temperature region, always keeping NO_x conversion around 90% even with the high value of GHSV used in this study (Figure 5B). The Fe-ZSM5 was however very sensitive to standard SCR conditions [42] and NO_x conversion significantly decreased when the NO_2/NO_x ratio was lower than 0.5. The NO_x conversion activity and the obtained trends over Fe-ZSM5 are comparable to the ones reported in literature under similar

reaction conditions [13,16,42-44] and are compared in Table S1. The presence of soot was not significant for the SCR reaction due to the fact that the SCR reaction was kinetically much faster compared to the soot oxidation. Slightly lower NO_x conversions were obtained due to slightly lowered NO_2 concentration which was used for the soot oxidation. The N_2 selectivity was also high in the whole range (>95%) and N_2O production was always lower than 10 ppm (Figures 5B and S6).

3.4. Catalytic activity of the integrated soot oxidation and NO_x SCR reactions

3.4.1. Soot oxidation activity of the integrated soot oxidation and NO_x SCR reactions

By mixing our soot oxidation catalyst (KCZ) with the SCR catalyst (Fe-ZSM5), the soot oxidation was significantly improved (Figure 6A). However, the contact mode between the SCR and soot oxidation catalyst played a major role. The best soot oxidation activity was obtained when the KCZ catalyst was in powdered form and the SCR in pellets, as the best contact between the soot oxidation catalyst and soot was achieved. In this case, the soot oxidation profile was comparable to the profile of soot oxidation in only O_2, since NO_2 was converted by the SCR catalyst. A small portion was however still segregated from the KCZ. This is indicated through T_{10} and T_{50} which were practically the same as with soot oxidation on KCZ in O_2. T_{90} was however much higher in the physical mixture configuration, i.e. it was more difficult to completely burn all the soot. This also confirmed that in the physical mixture configuration, without strong NO to NO_2 oxidation, the NO_x played no significant role in soot oxidation since it was consumed by the SCR reaction. In contrast, when the KCZ catalyst was in pellets and Fe-ZSM5 in powdered form only a small initial catalytic activity was observed. Since Fe-ZSM5 acted like a physical barrier there was little contact between KCZ and soot and most of the soot was burned by non-catalytic thermal oxidation. The worst result was obtained by co-pelletizing the Fe-ZSM5 and KCZ; by this way the catalytic soot oxidation was significantly inhibited. From the above results, we can conclude that when soot is mixed in loose contact with both KCZ and Fe-ZSM5 the effective range of KCZ is not higher than few μms [45] and if the soot oxidation catalyst is not powdered (well dispersed) soot is physically segregated from KCZ by the

SCR catalyst. In general, the catalytic soot oxidation activity is related more to the external morphology of the catalyst while the specific surface area has little influence [11, 28,29,39]. Catalyst morphology with shapes that contribute to formation of active oxygen and increased contact points with soot, e.g. nanocubes, nanorods, etc, have better soot oxidation performance [11,28,29,39]. As can be seen on the SEM images on figure S2 the CZ surface was coated with the potassium compounds (carbonates, hydroxides and nitrates). In several studies it was highlighted that these salts can form melts on the surface which in turn improves the soot-catalyst contact [9,26,27]. In the physical mixture the granulation was more important as the SCR catalyst, when in powdered form (diameter <100 μm), presented a barrier and prevented the soot-soot oxidation catalyst contact. When KCZ was saturated and used in pellets and Fe-ZSM5 in powder, the release and increased reactivity of NO_x on KCZ-sat enabled high initial soot oxidation rate. However, once the nitrates were depleted from the catalyst, the oxidation rate dropped significantly, and the second portion of soot was oxidized without significant enhancement deriving from the NO_x.

In the dual-bed reactor configuration, the SCR reaction had no effect on soot oxidation since the distance between the two layers (c.a. 3 mm) was too large and diffusion played no role (see above the Pe number). During soot oxidation NO_x could be utilized and the best results were obtained for this type of setup. Considering however the distances between the two layers on the potential SCR^2F (in the range of few μms) the dual bed reactor setup is not representative, and it more closely resembles a separate two-unit system.

From these findings, we can infer that the monolith coating method with the soot oxidation catalyst would be a key factor. A thin uniform KCZ layer coated on the top of the monolith wall would provide the best contact with soot. Deposition inside the pores with the SCR catalyst would likely have negative effect since it would only increase the pressure drop, while the contact with soot would be minimal [8].

During the soot oxidation by employing only Fe-ZSM5, the selectivity towards CO_2 was low (only 52%) and the CO concentration was high. For this reason, in commercial systems SCRoF must be

followed by an oxidation catalyst. In contrast, with the physical mixture configuration, the CO_2 selectivity remained high during the reaction (>90%) and this would eliminate the need for another oxidation aftertreatment unit.

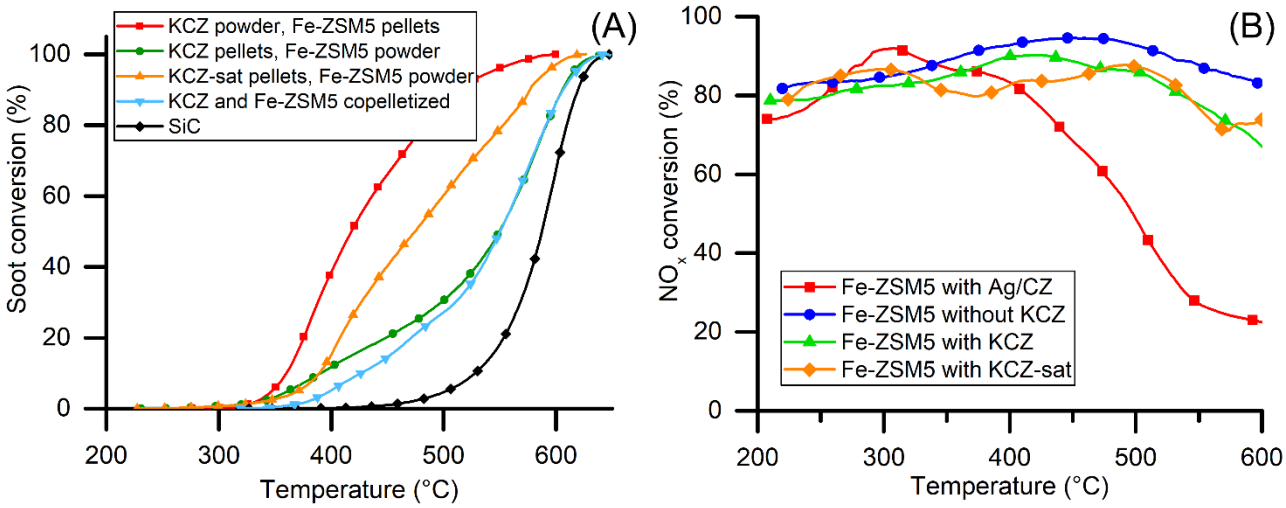

Figure 6. A) Soot oxidation in the physical mixture configuration. B) Corresponding SCR activity in the physical mixture configuration. Reaction conditions: *w/f* 0.054 g_{cat}·s/mL, 250 ppm NO, 250 ppm NO_2 and/or 500 ppm NH_3 4% O_2 in N_2, 9:9:1 KCZ: Fe-ZSM5: soot mass ratio, loose contact, 2 °C/min heating ramp.

Table 3. Soot oxidation on Fe-ZSM5 and KCZ physical mixture configuration with different granulation. Reaction conditions same as in Fig 6.

Configuration	T_{10} [°C]	T_{50} [°C]	T_{max} [°C]	T_{90} [°C]	CO_2 selectivity[a] [%]	Specific soot oxidation rate[b]
Fe-ZSM5 powder, KCZ pellet	390	550	585	605	89	0.59
Fe-ZSM5 pellet, KCZ powder	360	418	377	510	94	2.90
Fe-ZSM5 powder, KCZ-sat pellet	390	402	474	575	93	2.89
Fe-ZSM and KCZ pelletized together	426	550	590	604	84	0.67
Dual bed reactor configuration	354	398	355	445	94	3.79
Fe-ZSM5 with Ag/CZ	375	446	454	513	99	1.69
SiC	528	587	594	620	51	0

[a]CO_2 selectivity at T_{max}
[b]The specific soot oxidation rate was calculated at 400 °C and expressed as [$mg_{oxidized\ soot} \cdot s^{-1} \times g_{initial\ soot} \cdot g^{-2}_{catalyst}$]

3.4.2. SCR activity of the integrated soot oxidation and NO_x SCR reactions

Figure 6B illustrates the NO_x conversion in the physical mixture configuration. The addition of powdered KCZ to the mixture slightly decreased the NO_x conversion by ca. 3-5% compared to the case of Fe-ZSM5 without KCZ. This was most likely because the KCZ was catalytically active for the soot-NO_2 reaction rate and slightly lowered the NO_2/NO_x ratio. As shown in Figure S4, the NO_2/NO_x ratio during soot oxidation on KCZ decreased which in turn had negative influence on the SCR reaction. This deviation in NO_2/NO_x ratio from the ideal 0.5 means that the fast SCR was partially inhibited. Only at temperatures above 550 °C there was a significant decrease in NO_x conversion, however this was only due to the desorption of NO (see NO_x-TPDO in Figure 2B).

In order to reproduce the "worst-case scenario" for the NO_x conversion, the KCZ soot oxidation catalyst was saturated with NO_x before the test. With KCZ-Sat the pre-adsorbed NO_x was released during the continuous temperature increase. A drop in the NO_x conversion was observed at temperatures corresponding to the peaks in the NO_x TPDO at 360 °C and 440 °C (see Figure 2B). This temporary decrease in the NO_x conversion was modest (ca. 12%) and it was never lower than 70%. After the release of all the NO_x from the KCZ-sat, the conversion returned to the original value. In real application, the NO_x adsorption on the potassium could have positive effect in dynamic conditions since it would store NO_x at high concentration and low temperatures when the SCR catalyst is less active and releasing it during higher temperatures when NO_x conversion and soot oxidation rate is higher. The addition of basic component to induce inertia in NO_x emission was shown recently by [49] for physical mixture of Ba/Al_2O_3 and Cu-zeolite to be highly beneficial for reducing cold start emissions. In the dual bed reactor configuration, the KCZ-sat in the upper layer had no significant effect on the subsequent SCR reaction and the NO_x conversion was the same as in the physical mixture of Fe-ZSM5 with KCZ-sat.

By using the Ag/CZ catalyst the SCR reaction could not proceed because ammonia was oxidized (Figure 6B). At lower temperature, when there was excess NH_3, high N_2O production was observed and the selectivity was lowered (Figure S6). At higher temperatures, the NO_x conversion decreased significantly, because the ammonia oxidation on Ag/CZ was competitive with SCR. This highlights the importance that the soot oxidation catalyst used in the proposed dual layer catalyst SCR^2F configuration should be inert towards ammonia.

3.5. Stability of KCZ catalyst

The catalyst showed satisfactory low-temperature stability in the repeated soot combustion and after 6 cycles the T_{50} was increased by only 23 °C (see Table 4). The difference in the onset of the soot oxidation was however more pronounced, T_{10} increasing by 42 °C.

The high temperature and harsh hydrothermal ageing lowered the soot oxidation rate compared to fresh KCZ and T_{50} increased by 115 °C. The FE-SEM analysis revealed that, under hydrothermal conditions, the potassium tends to recrystallize and form aggregates. This causes the loss of contact between the support and the potassium and the positive synergistic effect is lost. However, the activity remaining after the harsh treatment was still significant and comparable to soot oxidation catalysts in the literature (Table 1 or e.g. [47]).

Table 4. Stability of the KCZ catalyst under different conditions

Configuration	T_{10} [°C]	T_{50} [°C]	T_{max} [°C]	T_{90} [°C]	CO_2 selectivity[a] [%]	Specific soot oxidation rate[b]
CZ	526	579	586	610	63	0
Fresh KCZ	348	417	429	470	93	2.91
Hydrothermally aged KCZ	454	532	560	580	93	1.37
KCZ 3rd run	368	426	432	481	92	2.51
KCZ 6th run	390	440	440	497	92	2.38

[a]CO_2 selectivity at T_{max}

[b]The specific soot oxidation rate was calculated at 400 °C and expressed as [$mg_{oxidized\ soot} \cdot s^{-1} \times g_{initial\ soot} \cdot g^{-2}_{catalyst}$]

4. Conclusions

It has been demonstrated that soot oxidation can be integrated on SCRoF by using specifically tailored soot oxidation catalyst, which is inactive towards ammonia oxidation. When only Fe-ZSM5 (an SCR catalyst) was used, the soot oxidation was inhibited by the SCR reaction because NO_2 was not available. In general, in SCRoF the strategy of soot oxidation by NO_x cannot be exploited because of the fast SCR reaction is consuming most of the NO_2.

The soot oxidation catalyst used in this study was potassium based. 20 wt.% potassium carbonate impregnated on CeO_2-ZrO_2 had strong synergistic effect with the support and high activity for soot oxidation with O_2. Furthermore, the addition of potassium poisoned the acid sites of the support and inhibited any ammonia reactivity. By physically mixing the SCR catalyst (Fe-ZSM5) and the soot oxidation catalyst (KCZ), activity of soot oxidation was successfully coupled with ammonia-mediated NO_x reduction. In the physical mixture, KCZ had no negative effect for NO_x reduction, while the Ag/CZ, employed for comparison, inhibited the SCR reaction by oxidizing ammonia, thereby lowering selectivity and conversion.

In the physical mixture the contact and granulation mode played a significant role for the soot oxidation activity and the best results were obtained when KCZ was powdered and Fe-ZSM5 pelletized. In the reversed case, powdered Fe-ZSM5 acted as a barrier between soot and KCZ and the soot oxidation was inhibited. This has further implication for the monolith coating method, i.e. the contact between soot oxidation catalyst with soot should be maximized and that with the SCR catalyst minimized.

It should be noted that in this study the catalytic activities and interactions were studied on powdered catalysts. While the length-scales (order of magnitude ~100 μm) and diffusion phenomena are similar as in a monolith, the interaction described are mainly of chemical nature, i.e. the reactivity, adsorption-desorption phenomena etc. Further studies on real monolith will be performed to describe the macroscopic physical phenomena since the addition of a soot oxidation coating layer on the

monolith would most likely have significant effect on the diffusion rate of the reacting species and the pressure drop through the monolith wall.

References

[1] Schejbal M, Stepanek J, Marek M, Koci P, Kubicek M (2010) Fuel 89:2365.

[2] Tomić MD, Savin LD, Mićić RD, Simikić MD, Furman TF (2013) Therm. Sci. 17:263.

[3] Shigapov A, Dubkov A, Ukropec R, Carberry B, Graham G, Chun W, McCabe R (2008) Kinet. Catal. 49:756.

[4] Tang W, Youngren D, SantaMaria M, Kumar S (2013) SAE Int. J. Engines 6:862.

[5] Watling TC, Ravenscroft MR, Avery G (2012) Catal. Today 188:32.

[6] Lapuerta M, Oliva F, Agudelo JR, Boehman AL (2012) Combust. Flame 159:844.

[7] Karamitros D, Koltsakis G (2017) Chem. Eng. Sci. 173:514.

[8] Rappé KG (2014) Ind. Eng. Chem. Res. 53:17547.

[9] Neyertz CA, Miró EE, Querini CA (2012) Chem. Eng. J. 181–182:93.

[10] Weng D, Li J, Wu X, Si Z (2011) J. Environ. Sci. 23:145.

[11] Kumar PA, Tanwar MD, Bensaid S, Russo N, Fino D (2012) Chem. Eng. J. 207-208:258.

[12] Corro G, Flores A, Pacheco-Aguirre F, Pal U, Bañuelos F, Ramirez A, Zehe A (2019) Fuel 250:17.

[13] Metkar PS, Harold MP, Balakotaiah V (2012) Appl. Catal. B Environ. 111:67.

[14] Wittka T, Holderbaum B, Dittmann P, Pischinger S (2015) Emiss. Control Sci. Technol. 1:167.

[15] Myung CL, Jang W, Kwon S, Ko J, Jin D, Park S (2017) Energy 132:356.

[16] Bensaid S, Balakotaiah V, Luss D (2017) AIChE J. 63:238.

[17] Mihai O, Tamm S, Stenfeldt M, Olsson L (2016) Philos. Trans. R. Soc. A Math. Phys. Eng. Sci. 374:20150086.

[18] Marchitti F, Nova I, Tronconi E (2016) Catal. Today. 267:110.

[19] Czerwinski J, Zimmerli Y, Mayer A, D'Urbano G, Zürcher D (2015) Emiss. Control Sci. Technol. 1:152.

[20] Park SY, Narayanaswamy K, Schmieg SJ, Rutland CJ (2012) Ind. Eng. Chem. Res. 51:15582.

[21] Wolff T, Deinlein R, Christensen H, Larsen L (2014) SAE Int. J. Mater. Manuf. 7:671.

[22] Shimokawa H, Kurihara Y, Kusaba H, Einaga H, Teraoka Y (2012) Catal. Today 185:99.

[23] Davies C, Thompson K, Cooper A, Golunski S, Taylor SH, Bogarra Macias M, Doustdar O, Tsolakis A (2018) Appl. Catal. B Environ. 239:10.

[24] Jiménez R, García X, Cellier C, Ruiz P, Gordon AL (2006) Appl. Catal. A Gen. 297:125.

[25] Zhang Y, Su Q, Li Q, Wang Z, Gao X, Zhang Z (2011) Chem. Eng. Technol. 34:1864.

[26] Ogura M, Kimura R, Ushiyama H, Nikaido F, Yamashita K, Okubo T (2014) ChemCatChem. 6:479.

[27] Li Q, Wang X, Xin Y, Zhang Z, Zhang Y, Hao C, Meng M, Zheng L, Zheng L (2014) Sci. Rep. 4:4725.

[28] Yang Z, Hu W, Zhang N, Li Y, Liao Y (2019) J. Catal. 337:98.

[29] Aneggi E, Divins N, Leitenburg C, Llorca J, Trovarelli A (2014) J. Catal. 312:191.

[30] Mizutani K, Takizawa K, Shimokawa H, Suzawa T, Ohyama N (2013) Top. Catal. 56:473.

[31] Bisaiji Y, Yoshida K, Inoue M, Umemoto K, Fukuma T (2011) SAE Int. J. Fuels Lubr. 5:380.

[32] Hou N, Zhang Y, Meng M (2013) J. Phys. Chem. C. 117:4089.

[33] Wang Q, Sohn JH, Park SY, Choi JS, Lee JY, Chung JS (2010) J. Ind. Eng. Chem. 16:68.

[34] Peng Y, Li J, Huang X, Li X, Su W, Sun X, Wang D, Hao J (2014) Environ. Sci. Technol. 48:4515.

[35] Sánchez BS, Querini CA, Miró EE (2011) Appl. Catal. A Gen. 392:158.

[36] Matarrese R, Aneggi E, Castoldi L, Llorca J, Trovarelli A, Lietti L (2016) Catal. Today. 267:119.

[37] Castoldi L, Artioli N, Matarrese R, Lietti L, Forzatti P (2010) Catal. Today 157:384.

[38] Sinhamahapatra A, Jeon JP, Kang J, Han B, Yu JS (2016) Sci. Rep. 6:27218.

[39] Guillén-Hurtado N, García-García A, Bueno-López A (2013) J. Catal. 299:181.

[40] Castoldi L, Matarrese R, Lietti L, Forzatti P (2006) Appl. Catal. B Environ. 64:25.

[41] Peralta MA, Zanuttini MS, Ulla MA, Querini CA (2011) Appl. Catal. A Gen. 399:161.

[42] Iwasaki M, Shinjoh H (2010) Appl. Catal. A Gen. 390:71.

[43] Metkar PS, Harold MP, Balakotaiah V (2013) Chem. Eng. Sci. 87:51.

[44] Kamasamudram K, Currier N, Szailer T, Yezerets A (2010) SAE Int. J. Fuels Lubr. 3:664.

[45] Kamatani K, Higuchi K, Yamamoto Y, Arai S, Tanaka N, Ogura M (2015) Sci. Rep. 5:10161.

[46] Selleri T, Gramigni F, Nova I, Tronconi E, Dieterich S, Weibel M, Schmeisser V (2018) Catal. Sci. Technol. 8:2467.

[47] Fino D, Bensaid S, Piumetti M, Russo N (2016) Appl. Catal. A Gen. 509:75.